Important Notice to Authors

No further publication processing will occur until we receive your response to this proof.

Attached is a PDF proof of your forthcoming article in PRA. Your article has 11 pages and the Accession Code is **AS12227**.

Please note that as part of the production process, APS converts all articles, regardless of their original source, into standardized XML that in turn is used to create the PDF and online versions of the article as well as to populate third-party systems such as Portico, Crossref, and Web of Science. We share our authors' high expectations for the fidelity of the conversion into XML and for the accuracy and appearance of the final, formatted PDF. This process works exceptionally well for the vast majority of articles; however, please check carefully all key elements of your PDF proof, particularly any equations or tables.

Figures submitted electronically as separate files containing color appear in color in the online journal. However, all figures will appear as grayscale images in the print journal unless the color figure charges have been paid in advance, in accordance with our policy for color in print (https://journals.aps.org/authors/color-figures-print).

Specific Questions and Comments to Address for This Paper

1 The paper was edited throughout for clarity and formatted per style: Please check all changes carefully to ensure that meaning was not altered (note that some formatting changes are not marked to avoid cluttering the paper). Note that acronyms should be defined (only) at first use and must be used at least once after definition (in both the Abstract and the main text): Please check definitions inserted at first use.
2 Acknowledgments were modified per style: Please check.
3 Please update all arXiv references if possible.
4 Please update [12] or clarify if this is unpublished.
5 Please clarify publisher name and location in [14].
6 Please list full book title in [45].
FQ: This funding provider could not be uniquely identified during our search of the FundRef registry (or no Contract or Grant number was detected). Please check information and amend if incomplete or incorrect.
Q: This reference could not be uniquely identified due to incomplete information or improper format. Please check all information and amend if applicable.

ORCIDs: Please follow any ORCID links () after the authors' names and verify that they point to the appropriate record for each author. Requests to add ORCIDs should be sent no later than the first proof revisions. See complete details regarding ORCID requests and ORCID verification at https://journals.aps.org/authors/adding-orcids-during-proof-corrections.
NOTE: If this paper is an Erratum or a Reply, the corresponding author's ORCID may be present if previously provided to APS, but no ORCIDs can be added at proof stage.

Crossref Funder Registry ID: Information about an article's funding sources is now submitted to Crossref to help you comply with current or future funding agency mandates. Crossref's Funder Registry (https://www.crossref.org/services/funder-registry/) is the definitive registry of funding agencies. Please ensure that your acknowledgments include all sources of funding for your article following any requirements of your funding sources. Where possible, please include grant and award ids. Please carefully check the following funder information we have already extracted from your article and ensure its accuracy and completeness:
Fundação de Amparo à Ciência e Tecnologia do Estado de Pernambuco, BFP-0168-1.05/19, BFP-0115-1.05/21

Other Items to Check

- Please note that the original manuscript has been converted to XML prior to the creation of the PDF proof, as described above. Please carefully check all key elements of the paper, particularly the equations and tabular data.
- Title: Please check; be mindful that the title may have been changed during the peer-review process.
- Author list: Please make sure all authors are presented, in the appropriate order, and that all names are spelled correctly.
- Please make sure you have inserted a byline footnote containing the email address for the corresponding author, if desired. Please note that this is not inserted automatically by this journal.
- Affiliations: Please check to be sure the institution names are spelled correctly and attributed to the appropriate author(s).
- Receipt date: Please confirm accuracy.
- Acknowledgments: Please be sure to appropriately acknowledge all funding sources.
- Hyphenation: Please note hyphens may have been inserted in word pairs that function as adjectives when they occur before a noun, as in "x-ray diffraction," "4-mm-long gas cell," and "*R*-matrix theory." However, hyphens are deleted from word pairs when they are not used as adjectives before nouns, as in "emission by x rays," "was 4 mm in length," and "the *R* matrix is tested."

  Note also that Physical Review follows U.S. English guidelines in that hyphens are not used after prefixes or before suffixes: superresolution, quasiequilibrium, nanoprecipitates, resonancelike, clockwise.

- Please check that your figures are accurate and sized properly. Make sure all labeling is sufficiently legible. Figure quality in this proof is representative of the quality to be used in the online journal. To achieve manageable file size for online delivery, some compression and downsampling of figures may have occurred. Fine details may have become somewhat fuzzy, especially in color figures. The print journal uses files of higher resolution and therefore details may be sharper in print. Figures to be published in color online will appear in color on these proofs if viewed on a color monitor or printed on a color printer.
- Please check to ensure that reference titles are given as appropriate.
- Overall, please proofread the entire *formatted* article very carefully. The redlined PDF should be used as a guide to see changes that were made during copyediting. However, note that some changes to math and/or layout may not be indicated.

Ways to Respond

- ***Web:*** If you accessed this proof online, follow the instructions on the web page to submit corrections.
- ***Email:*** Send corrections to praproofs@aptaracorp.com
  Subject: **AS12227** proof corrections
- ***Fax:*** Return this proof with corrections to +1.703.791.1217. Write **Attention:** PRA Project Manager and the Article ID, **AS12227**, on the proof copy unless it is already printed on your proof printout.

PHYSICAL REVIEW A **00**, 002600 (2022)

Pauli component erasing quantum channels

José Alfredo de León,[1,2] Alejandro Fonseca,[3,2] François Leyvraz,[4] David Davalos,[5] and Carlos Pineda[2,*]

[1]*Instituto de Investigación en Ciencias Físicas y Matemáticas, Universidad de San Carlos de Guatemala, Ciudad Universitaria, Guatemala 01012, Guatemala*

[2]*Instituto de Física, Universidad Nacional Autónoma de México, Ciudad de México 01000, Mexico*

[3]*Departamento de Física, CCEN, Universidade Federal de Pernambuco, Recife 50670-901, PE, Brazil*

[4]*Instituto de Ciencias Físicas, Universidad Nacional Autónoma de México, Cuernavaca 62210, Mexico*

[5]*Institute of Physics, Slovak Academy of Sciences, Dúbravská cesta 9, Bratislava 84511, Slovakia*

(Received 16 May 2022; accepted 2 September 2022; published xxxxxxxxxx)

Decoherence of quantum systems is described by quantum channels. However, a complete understanding of such channels, especially in the multiparticle setting, is still an ongoing difficult task. We propose the family of quantum maps that preserve or completely erase the components of a multiqubit system in the basis of Pauli strings, which we call *Pauli component erasing maps*. For the corresponding channels, it is shown that the preserved components can be interpreted as a finite vector subspace, from which we derive several properties and complete the characterization. Moreover, we show that the obtained family of channels forms a semigroup and derive its generators. We use this simple structure to determine physical implementations and connect the obtained family of channels with Markovian processes.

DOI: 10.1103/PhysRevA.00.002600

I. INTRODUCTION

Quantum correlations [1–3], including entanglement [4], are an important resource for a wide variety of tasks that include teleportation [5], quantum computation [6], and others [7]. However, this resource is also extremely delicate [6,8], especially for multiparticle systems [4]; that is why an important part of the efforts of the community implementing quantum technologies is devoted to tackle this issue from an experimental [9,10] and theoretical [11–13] point of view. The process by which quantum correlations are unintentionally dissipated is called *decoherence* [8,14]. One of the main tools to study the effects of decoherence are quantum channels. Quantum channels can describe quantum noise [15,16], open quantum systems dynamics [6,17], and recently even coarse graining [18,19]. One of the main difficulties in characterizing quantum channels is that, like for quantum states, the number of parameters required for their description increases quite rapidly with Hilbert-space dimension. Moreover, such parameters are constrained in a complicated way by physical conditions, such as complete positivity [20]. Describing in detail families of channels having a given property provides insight into the jungle of quantum operations. For the qubit case there are several studies concerning the unital case, for which nontrivial properties can be described using only three parameters, which in turn form the well-known tetrahedron of Pauli channels [15,16,21]. More generally, in Ref. [22] the authors study families of convex combinations of quantum-classical channels that relate to unital qubit channels with positive eigenvalues, and give a generalization of the Bloch sphere. Similarly, a generalization of Pauli channels based on mutually unbiased measurements is introduced and studied in Ref. [23]. Other studies of channels beyond the qubit can be found [24–27].

In this paper we present a generalization of idempotent Pauli channels—i.e., the qubit flip operations (bit, phase, and bit phase when the flip probability is $1/2$), total depolarizing qubit channels, and the identity channel—to the case of N qubits. The generalization is done by extending Pauli observables to *Pauli strings* (tensor products of Pauli matrices) [28,29]. The resulting maps are unital and diagonal in the Pauli strings' basis. We shall in the following refer to such maps as *Pauli component erasing* (PCE) *maps*.

The main task which we perform in this paper is the identification of the conditions which an arbitrary PCE map must satisfy in order to be completely positive. The answer turns out to involve a strikingly simple and unexpected mathematical structure that is exploited to gain deeper understanding on aforementioned channels, as we show in Sec. III B. This structure allows us, for example, to describe such channels with a much reduced set of parameters (as compared to specifying a list of all erased Pauli components) or to define an interesting semigroup structure on the set of all PCE channels. Additionally, these channels are, in a sense, the simplest possible channels, and as such can be used as building blocks of more general channels. For instance, one can combine them (through convex superposition) or compose them with unitary transformations. To summarize succinctly the final result, we show that it is possible to assign to every Pauli string a simple PCE channel, obtained by extending the system with an ancilla of a single qubit, acting on the combined system by a unitary involving the Pauli string and tracing over the ancilla.

*carlospgmat03@gmail.com

 ©2022 American Physical Society

It then follows from our results that *all* PCE channels arise from such channels by composition.

The paper is organized as follows. In Sec. II we recall the properties of quantum channels needed to proceed with the definition of PCE maps. In Sec. III we diagonalize analytically the Choi matrix for arbitrary PCE maps and characterize their complete positivity by interpreting PCE quantum channels as finite vector subspaces. We study the generators of the semigroup structure associated to the set of PCE channels in Sec. IV, and we use them to derive meaningful physical interpretations of PCE channels in Sec. V, as well as Kraus operators of the generators. To finish, we conclude and discuss future perspectives and possible generalizations in Sec. VI.

II. PAULI COMPONENT ERASING MAPS

In this section we introduce the family of PCE maps. Let us start our discussion with a brief review of several basic concepts of quantum channels that will allow us to introduce some notation, and finish with the definition of PCE maps and some generalities. We further introduce a useful graphical representation for them.

A. Quantum channels

Quantum channels are the most general linear operations that a quantum system undergoes independently of its past [20,30]. The physical system under study will be associated with a Hilbert space denoted by H, and the set of linear operators over such space will be denoted by $\mathcal{B}(\mathsf{H})$. That way, a density matrix ρ of such system is an element of $\mathcal{B}(\mathsf{H})$.

The construction of quantum channels includes basically three ingredients: linearity, trace preservation, and complete positivity. Linearity is needed to map every convex combination of density matrices into a convex combination of the evolution of such density matrices. The trace preserving property is required for the process $\mathcal{E}$ to happen with probability 1, and reads $\mathrm{tr}\mathcal{E}[\rho] = \mathrm{tr}\rho = 1$. The complete positivity condition is needed to preserve positive semidefiniteness and handle the nonlocal nature of quantum theory. A linear map $\mathcal{E}$ is positive if it maps density operators to density operators, i.e., if $\mathcal{E}[\rho] \geqslant 0$ for all density matrices ρ. On the other hand, if one extends a positive map to include an ancilla, the resulting map is not always positive. If, for an ancillary system of arbitrary dimension, such extension results in a positive map, we say that the original map is completely positive [31]. Quantum channels are required to be completely positive so as to allow the proper evolution of potentially entangled states with an ancilla; to test this condition we require some additional steps.

A simple algorithm to test the complete positivity of a quantum channel was developed by Jamiokowski [32] and Choi [33]. One first exploits the isomorphism that maps a channel $\mathcal{E}$ to the state $\mathcal{D} = (\mathrm{id} \otimes \mathcal{E})[|\Omega\rangle\langle\Omega|]$, where $|\Omega\rangle = 1/\dim(\mathsf{H}) \sum_i^{\dim(\mathsf{H})} |i\rangle|i\rangle$ is a maximally entangled state between the original system and an ancilla and "id" is the identity channel. Remarkably, the map $\mathcal{E}$ is completely positive if and only if $\mathcal{D}$ (also called the Choi or dynamical matrix of $\mathcal{E}$) is positive semidefinite [32,33].

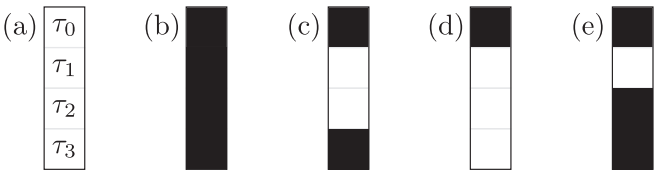

FIG. 1. In (a) we introduce the notation in the diagrams that represent the single-qubit PCE maps, so that each square corresponds to a single τ_α, $\alpha = 0, 1, 2, 3$. The diagrams in (b), (c), and (d) correspond to the identity map, completely dephasing channel, and complete depolarization, respectively, as the color of each square indicates the value attained by the corresponding τ_α, either 0 (white) or 1 (black). In (e) we show a map that only erases the component r_1, collapsing the Bloch sphere into a disk, and thus does not correspond to a quantum channel.

B. Structure of PCE maps

We have discussed the main features of quantum channels, and now we turn our attention to introduce the Pauli component erasing maps. We start by exploring the single-qubit scenario and then we treat the N-qubit case.

The most general single-qubit density matrix can be written as

$$\rho = \frac{1}{2}\sum_{\alpha=0}^{3} r_\alpha \sigma_\alpha, \tag{1}$$

with $\sigma_0 = \mathbb{1}$, and $\sigma_{1,2,3}$ the usual Pauli matrices. Normalization requires that $r_0 = 1$ and the remaining $r_{1,2,3}$ form the Bloch vector. Consider the map that projects each component in the following way:

$$r_\alpha \mapsto \tau_\alpha r_\alpha \tag{2}$$

where τ_α is either 0 or 1 (trace preserving requires that $\tau_0 = 1$). From now on we refer to any operation like that described in Eq. (2), as a PCE map. Not every such operation is a quantum channel; for example, collapsing the entire Bloch ball to a disk on the xy plane ($\tau_1 = \tau_2 = 1$ and $\tau_3 = 0$) leads to a violation of the CP conditions. Indeed, a direct evaluation of such conditions yields [15,20]

$$\begin{aligned} &1 + \tau_1 + \tau_2 + \tau_3 \geqslant 0, \\ &1 + \tau_\alpha - \tau_\beta - \tau_\gamma \geqslant 0 \ \ \forall\, \alpha \neq \beta \neq \gamma, \end{aligned} \tag{3}$$

where trace preserving is already imposed, and shows that five out of the eight one-qubit PCE maps are quantum channels. These operations are the identity map, the completely depolarizing channel ($\rho \mapsto \mathbb{1}/2$), and bit, phase, and bit-phase flip (with flip probability of $1/2$) channels [34], and can be pictured using one column tables showing the positions of 0s and 1s (see Fig. 1).

In order to present and develop the N-qubit case, it is useful to introduce the so-called Pauli strings, defined as

$$\sigma_{\vec{\alpha}} = \sigma_{\alpha_1} \otimes \sigma_{\alpha_2} \otimes \cdots \otimes \sigma_{\alpha_N}, \tag{4}$$

where $\vec{\alpha}$ denotes a multi-index $(\alpha_1, \ldots, \alpha_N)$ and $\alpha_i = 0, 1, 2, 3$. These Hermitian operators form an orthogonal basis in the space of operators acting on N qubits. In fact, $\mathrm{tr}\sigma_{\vec{\alpha}}\sigma_{\vec{\alpha}'} = 2^N \delta_{\vec{\alpha}\vec{\alpha}'}$ and $\mathrm{tr}\sigma_{\vec{\alpha}} = 2^N \delta_{\vec{\alpha}\vec{0}}$.

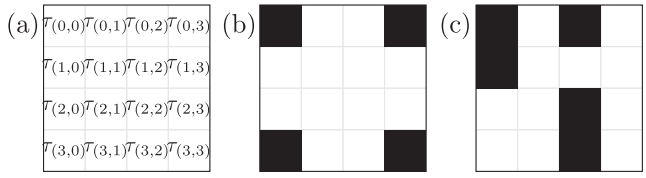

FIG. 2. In (a) we introduce the positions of two qubit diagrams. The diagram in (b) corresponds to a quantum channel that results from the tensor product of bit flip channels in each qubit [see Fig. 1(c)], and in (c) a diagram of a map that is not a quantum channel is presented.

Similarly to the single-qubit case, the density matrix ρ of a system of N qubits can be written using Pauli strings in the following way:

$$\rho = \frac{1}{2^N}\sum_{\vec{\alpha}} r_{\vec{\alpha}}\sigma_{\vec{\alpha}}, \tag{5}$$

so $r_{\vec{\alpha}} = \langle\sigma_{\vec{\alpha}}\rangle = \mathrm{tr}(\rho\sigma_{\vec{\alpha}})$ is the coefficient corresponding to the expansion of the density matrix in the normalized basis of Pauli strings. Again, normalization of the state requires that $r_{\vec{0}} = 1$. We shall refer to $r_{\vec{\alpha}}$ as the *Pauli components* of the density matrix of a system of qubits.

In general, a PCE map is a map that either preserves or completely erases the Pauli components of a density matrix. That is,

$$r_{\vec{\alpha}} \mapsto \tau_{\vec{\alpha}} r_{\vec{\alpha}}, \quad \tau_{\vec{\alpha}} = 0, 1. \tag{6}$$

In addition, for the operation to be trace preserving, it is required that $\tau_{\vec{0}} = 1$. It is worth noticing that, as for the single-qubit case, not all PCE maps are quantum operations. On the other hand, constructing and evaluating the conditions for complete positivity is nontrivial and is the main problem addressed in this paper. We shall refer to the map $r_{\vec{\alpha}} \mapsto \tau_{\vec{\alpha}} r_{\vec{\alpha}}$, with arbitrary values of $\tau_{\vec{\alpha}}$ (only restricted by complete positivity), as *Pauli diagonal maps*.

A graphical representation for PCE maps may be introduced, being the two-qubit case that has proved to be the most useful. Consider a N-dimensional Cartesian grid, with 4^N places. Each place has N integer coordinates, ranging from 0 to 3, so each place corresponds to a given $\vec{\alpha}$ in Eq. (5). For a given PCE, we shall fill the square if the corresponding $\tau_{\vec{\alpha}} = 1$. Otherwise, we leave it empty. Examples for $N = 1$ and 2 are provided in Figs. 1 and 2, respectively.

It is worth noticing that the set of PCE maps overlaps with the set of "Pauli diagonal channels constant on axes" defined in Ref. [22], consisting of convex combinations of *quantum-classical* channels. In particular, it can be shown that quantum-classical channels defined with the eigenbasis of some set of $2^N - 1$ commuting Pauli observables [29] comprise a PCE map with exactly 2^N components equal to 1s in its diagonal. For details, we refer the reader to Appendix A.

III. MATHEMATICAL CONSIDERATIONS

This section is devoted to deriving the conditions a Pauli diagonal map needs to satisfy the complete positivity condition, i.e., that all the eigenvalues of the Choi matrix associated to the channel are non-negative. To do so, we calculate and diagonalize the Choi matrix of a general Pauli diagonal map, first for a single qubit and then for N qubits. Finally, we restrict from Pauli diagonal maps to PCE maps, and provide a connection between a vector subspace and the set of coefficients $\{\tau_{\vec{\alpha}}\}$ in Eq. (6) of a PCE quantum channel. This allows us to derive several important properties of this particular family of channels.

A. Diagonalization of the Choi matrix

We now construct the Choi matrix of a single-qubit Pauli diagonal map $\mathcal{E}$. As described above, $\mathcal{E}$ is a linear map from $\mathcal{B}(\mathsf{H})$ to itself. We shall denote elements of $\mathcal{B}(\mathsf{H})$ by the notation $|\cdot\rangle\rangle$. Thus, for instance, $|\sigma_\alpha\rangle\rangle$ represents the Pauli matrix σ_α understood as a vector belonging to $\mathcal{B}(\mathsf{H})$, for the present case, in which $\mathsf{H} = \mathbb{C}^2$. Since the scalar product in $\mathcal{B}(\mathsf{H})$ is given by $\langle\langle A_1|A_2\rangle\rangle = \mathrm{tr}A_1^\dagger A_2$, elements of the Pauli basis satisfy the relation $\langle\langle\sigma_\alpha|\sigma_{\alpha'}\rangle\rangle = \mathrm{tr}(\sigma_\alpha^\dagger\sigma_{\alpha'}) = 2\delta_{\alpha\alpha'}$. In this language, the state of a single qubit reads $|\rho\rangle\rangle = 2^{-1}\sum_{\alpha=0}^{3} r_\alpha |\sigma_\alpha\rangle\rangle$ and the matrix form of the map $\mathcal{E}$ is

$$\hat{\mathcal{E}} = \frac{1}{2}\sum_{\alpha=0}^{3}\tau_\alpha |\sigma_\alpha\rangle\rangle\langle\langle\sigma_\alpha|\,. \tag{7}$$

After some steps, detailed from Eq. (B3) to Eq. (B6), it is possible to show that the Choi matrix of $\mathcal{E}$ reads

$$\mathcal{D} = \frac{1}{2}\sum_{\alpha=0}^{3}\tau_\alpha\sigma_\alpha\otimes\sigma_\alpha^*. \tag{8}$$

Notice that $|\sigma_\alpha\rangle\rangle\langle\langle\sigma_\alpha|$ and $\sigma_\alpha\otimes\sigma_\alpha^*$ are different operators. Indeed, the former acts as a linear map upon the vector space $\mathcal{B}(\mathsf{H})$, whereas the latter acts on the tensor product $\mathsf{H}\otimes\mathsf{H}$. Of course, there is a basis dependent identification between these two spaces, which is used in the construction of the Choi matrix. Surprisingly, one can in fact show that $\mathcal{D}$ is diagonal in the Pauli basis (see Appendix B for details). The eigenvalues are

$$\lambda_\alpha = \frac{1}{2}\sum_{\beta=0}^{3} a_{\alpha\beta}\tau_\beta, \tag{9}$$

where

$$a = \begin{pmatrix} 1 & 1 & 1 & 1 \\ 1 & 1 & -1 & -1 \\ 1 & -1 & 1 & -1 \\ 1 & -1 & -1 & 1 \end{pmatrix}. \tag{10}$$

We wish to add that one can replace a with $H\otimes H$, with H the Hadamard matrix, and still diagonalize the same Choi matrix $\mathcal{D}$. This is due to the fact that a corresponds to a permutation of rows of $H\otimes H$. However, we chose the aforementioned definition as some later considerations [see Eq. (32)] cannot be easily written in terms of $H\otimes H$.

The same program can be carried out for N qubits. In this case, one uses the vectorized Pauli strings:

$$|\sigma_{\vec{\alpha}}\rangle\rangle = \left|\sigma_{\alpha_1}\otimes\cdots\otimes\sigma_{\alpha_N}\right\rangle\!\rangle. \tag{11}$$

This vectorization must not be confused with the tensor product of all $|\sigma_{\alpha_i}\rangle\rangle$, since the tensor product and the vectorization process generally do not commute [35]. The vectors satisfy

the orthogonality relation $\langle\langle\sigma_{\vec{\alpha}}|\sigma_{\vec{\alpha}'}\rangle\rangle = 2^N\delta_{\vec{\alpha}\vec{\alpha}'}$. The matrix representation of the map corresponding to a Pauli diagonal map is

$$\hat{\mathcal{E}}_N = \frac{1}{2^N}\sum_{\vec{\alpha}} \tau_{\vec{\alpha}}\, |\sigma_{\vec{\alpha}}\rangle\rangle\langle\langle\sigma_{\vec{\alpha}}|\,. \tag{12}$$

As in the previous case, the Choi matrix $\mathcal{D}_N$ may be written in terms of tensor products of Pauli matrices:

$$\mathcal{D}_N = \frac{1}{2^N}\sum_{\vec{\alpha}} \tau_{\vec{\alpha}} \bigotimes_{j=1}^{N} \sigma_{\alpha_j} \otimes \sigma^*_{\alpha_j}. \tag{13}$$

This matrix is again diagonal in the (multiqubit) Pauli basis, with the eigenvalue corresponding to $|\sigma_{\vec{\alpha}}\rangle\rangle$ given by

$$\lambda_{\vec{\alpha}} = \frac{1}{2^N}\sum_{\vec{\beta}} A_{\vec{\alpha}\vec{\beta}}\tau_{\vec{\beta}}, \tag{14}$$

where

$$A = a^{\otimes N}. \tag{15}$$

Again, the proofs are provided in Appendix B. We wish to add that we could diagonalize $\mathcal{D}_N$ with $H^{\otimes 2N}$ instead of $a^{\otimes N}$, which might be more convenient for other applications.

B. PCE quantum channels as vector spaces

In this subsection we will provide a one-to-one relation between PCE quantum channels and the subspaces of a discrete vector subspace associated with the indices $\vec{\alpha}$ labeling the components of a state [see Eq. (5)]. Some established facts about vector spaces will allow us to derive the main features of PCE quantum channels.

Let us start by recalling that the problem of determining complete positivity of a PCE map can be recast as determining which coefficients $\tau_{\vec{\alpha}}$ are mapped via A to positive eigenvalues $\lambda_{\vec{\alpha}}$, as in Eq. (14). Using the fact that $a^{-1} = a/4$, and so

$$A^{-1} = \frac{1}{4^N}A, \tag{16}$$

we can directly invert Eq. (14) to obtain

$$\sum_{\vec{\beta}} A_{\vec{\alpha}\vec{\beta}}\lambda_{\vec{\beta}} = 2^N\tau_{\vec{\alpha}}, \tag{17}$$

which will serve as a starting point for our analysis. This is a remarkable equation, as it provides a method to diagonalize the Choi matrix of any Pauli diagonal map.

Two other simple but crucial observations are the following. For valid quantum channels it holds that

$$\sum_{\vec{\alpha}\in\Omega}\lambda_{\vec{\alpha}} = 0 \quad\Rightarrow\quad \lambda_{\vec{\alpha}} = 0,\ \forall\vec{\alpha}\in\Omega \tag{18}$$

for an arbitrary subset of multi-indices Ω, as each member of the sum is greater than or equal to zero, due to complete positivity of the underlying channel. Finally, setting $\vec{\alpha} = 0$ in Eq. (17), and taking into account the normalization condition that $\tau_{\vec{0}} = 1$, we obtain

$$\sum_{\vec{\alpha}}\lambda_{\vec{\alpha}} = 2^N, \tag{19}$$

since $A_{\vec{0},\vec{\beta}} = 1$ for all $\vec{\beta}$.

Now we need a definition: to each multi-index $\vec{\alpha}$ we associate a *set* of multi-indices $\Phi(\vec{\alpha})$ as follows:

$$\Phi(\vec{\alpha}) = \{\vec{\beta} : A_{\vec{\alpha}\vec{\beta}} = 1\}. \tag{20}$$

If we now assume that $\tau_{\vec{\alpha}} = 1$, and calculate the difference between Eq. (19) and $\sum_{\vec{\beta}} A_{\vec{\alpha}\vec{\beta}}\lambda_{\vec{\beta}} = 2^N$ [which follows from Eq. (17) and $\tau_{\vec{\alpha}} = 1$], one obtains

$$\lambda_{\vec{\beta}} = 0, \quad \forall\vec{\beta}\notin\Phi(\vec{\alpha}). \tag{21}$$

Thus, if $\tau_{\vec{\alpha}} = 1$, then $\tau_{\vec{\gamma}}$ and $\tau_{\vec{\gamma}'}$ are equal if

$$A_{\vec{\beta}\vec{\gamma}} = A_{\vec{\beta}\vec{\gamma}'}, \quad \forall\vec{\beta}\in\Phi(\vec{\alpha}). \tag{22}$$

This follows from restricting the sum Eq. (17) to $\lambda_{\vec{\beta}} \neq 0$, given in Eq. (21). Condition (22) therefore connects three multi-indices, $\vec{\alpha}$, $\vec{\gamma}$, and $\vec{\gamma}'$. When such a connection exists, $\tau_{\vec{\alpha}} = 1$ implies $\tau_{\vec{\gamma}} = \tau_{\vec{\gamma}'}$.

Let us now work out the nature of the aforementioned connection. For arbitrary k we define a vector $\vec{\beta}_k$ such that $\vec{\beta}_k \in \Phi(\vec{\alpha})$ as follows: $\vec{\beta}_k$ is zero everywhere except for the kth coordinate, which takes a value β such that $a_{\alpha_k\beta} = 1$. Since $a_{\alpha 0} = 1$ for any α, this particular choice of $\vec{\beta}$ indeed belongs to $\Phi(\vec{\alpha})$, so that if Eq. (22) holds for all $\vec{\beta}\in\Phi(\vec{\alpha})$ it must hold for that particular $\vec{\beta}_k$, which leads to

$$a_{\beta\gamma_k} = a_{\beta\gamma'_k} \tag{23}$$

for all β such that $a_{\alpha_k\beta} = 1$. One can verify, by working out the different cases, that Eq. (23) is equivalently expressed as

$$\gamma'_k = \alpha_k \oplus \gamma_k \tag{24}$$

where $\oplus$ denotes the operation of the Klein group (see Table I for a detailed description).

TABLE I. Definition of the $\oplus$ operation [see Eq. (23)]. Note that the operation is an Abelian group; in fact it corresponds to the Klein group, where the neutral element is zero. This is the reason for choosing an additive notation for the operation defined in (23).

$\oplus$	0	1	2	3
0	0	1	2	3
1	1	0	3	2
2	2	3	0	1
3	3	2	1	0

It will be useful to think of the multi-index $\vec{\alpha}$ as an element of a vector space. To do so, we notice that any group with the property that $\alpha\oplus\alpha = 0$ is indeed a vector space under the two-element field $\{0, 1\}$. We notice that the Klein group described in Table I is actually isomorphic to the two-dimensional vector space over the field of two elements $\{0, 1\}$. Then, we build the complete vector space, with the same field, and defining $\vec{\alpha}\oplus\vec{\beta} = (\alpha_1\oplus\beta_1, \cdots, \alpha_N\oplus\beta_N)$ [36]. We can indeed restate Eq. (24) and say that, for quantum channels, if $\tau_{\vec{\alpha}} = 1$, then $\tau_{\vec{\gamma}} = \tau_{\vec{\alpha}\oplus\vec{\gamma}}$. For example, in Fig. 2(c) the indices

that correspond to preserved components are $\vec{\alpha}^{(0)} = (0, 0)$, $\vec{\alpha}^{(1)} = (0, 2)$, $\vec{\alpha}^{(2)} = (1, 0)$, $\vec{\alpha}^{(3)} = (2, 2)$, and $\vec{\alpha}^{(4)} = (3, 2)$. However, $\vec{\alpha}^{(1)} + \vec{\alpha}^{(2)} = (1, 2)$, which is not preserved, and thus this diagram does not correspond to a quantum channel. From this view we can derive several interesting observations that will be presented in the rest of the section.

From this readily follows an amusing property: the set of all multi-indices $\vec{\gamma}$ for which $\tau_{\vec{\gamma}} = 1$ is closed under binary vector addition; in other words, it forms a vector subspace of the set of all multi-indices. A moment's consideration will further show that the above reasoning can be inverted; that is, if we set all $\tau_{\vec{\gamma}}$ equal to 1 whenever $\vec{\gamma}$ belongs to a given vector subspace of the set of all indices, then τ indeed has an image which has only positive components. In other words, there is a one-to-one correspondence between a quantum channel, and a vector subspace of the aforementioned space.

With this information, we present a procedure to generate all solutions: we start out from the solution having $\tau_{\vec{0}} = 1$, with everything else zero. We may then successively switch $\tau_{\vec{\alpha}}$'s to 1 for various values of $\vec{\alpha}$, taking care immediately to set equal to 1 the components of τ that correspond to values of $\vec{\beta}$ generated by the previously switched values of $\vec{\alpha}$ via the operation $\oplus$. Doing so, in an ordered way, allows one to generate all PCE quantum channels with a given set of preserved components, without the need of exploring the exponentially large space of all PCE maps.

We can show that all PCE quantum channels preserve 2^K components. First recall that a vector space of dimension d over a field of q elements has q^d elements [37]. Now V is a vector space on a field of two elements having dimension $2N$. We have seen earlier that

$$W = \{\vec{\alpha} : \vec{\alpha} \in V, \tau_{\vec{\alpha}} = 1\} \tag{25}$$

is a subspace of V. As such, W has a given dimension K, which means that W has 2^K elements. In other words, a set of indices $\tau_{\vec{\alpha}}$ with the property discussed above can only have 2^K elements equal to 1, for a given integer K.

It is natural to ask how many PCE quantum channels exist that preserve 2^K components. One can calculate such number, $\mathcal{S}_{N,K}$, by examining the number of different independent subsets of vectors that spawn a given vector subspace. In Appendix C we show that

$$\mathcal{S}_{N,K} = \prod_{m=0}^{K-1} \frac{2^{2N-m} - 1}{2^{K-m} - 1}. \tag{26}$$

From the above expression, it is easy to see the symmetry relation

$$\mathcal{S}_{N,K} = \mathcal{S}_{N,2N-K} \tag{27}$$

which suggests a relation between individual channels that preserve K and $2N - K$ Pauli components that for the time being has escaped our efforts to identify.

Finally, let us point out the following: if we wish to specify a PCE channel explicitly, the naive way to proceed would be simply to list all the Pauli components which are not erased. This requires in general, however, an exponential amount of information: that is, if the system has N qubits, we generally require of the order of 2^N bits to do this. If, on the other hand, we take advantage of the vector space structure of a PCE channel, we only need to specify a basis. Since a basis consists of N vectors of length N, the information required is only of N^2 bits, so that we have obtained a very substantial improvement by exploiting complete positivity. This is reminiscent of a rather similar effect in *stabilizer states* which can also be specified by N^2 bits, as opposed to an exponentially large number of basis coefficients for arbitrary states. A stabilizer state is one which is the common eigenvector to the eigenvalue 1 of a set of N commuting Pauli strings. The similarity is highly intriguing, and potentially of interest, since stabilizer states are of central importance in quantum error correction [38].

IV. GENERATORS

We now discuss the existence of a generator set for all PCE quantum channels and how to label each of them uniquely as $\mathcal{G}_{\vec{\alpha}}$ (according to its local action on every qubit in the system). Finally we will discuss a symmetry of PCE quantum channel generators and a connection between them and A [see Eq. (15)].

There exists a subset of PCE quantum channels that generates the entire set; the nature of these generators may be studied, as we shall see, with the properties of the aforementioned vector space. By standard theorems of linear algebra, any proper subspace W [see Eq. (25)] can be extended to a maximal nontrivial subspace of dimension $2N - 1$ by adjoining appropriate additional basis elements. This can be done in different ways. We therefore arrive to the set of maximal extensions of W, where every maximal subspace corresponds to a PCE quantum channel that preserves half of the Pauli components. The intersection of all the elements of this set reduces to W itself, and since intersection of subspaces translates to composition of PCE channels this implies that all PCE quantum channels can be obtained as compositions of PCE channels corresponding to maximally nontrivial subspaces, plus the identity map. In other words, the set of PCE quantum channels that preserve half of the components plus the identity map is a generator set for all PCE channels. Consider Fig. 3; Figs. 3(c)–3(e) represent nontrivial PCE generators (PCEGs) and the composition of any two of them yields the PCE channel corresponding to Fig. 3(b).

A PCEG may be characterized by its local action on every qubit in the system. This action can be encoded using a multi-index $\vec{\alpha}$, as in (4), hence each of the different 4^N multi-indices may be uniquely related to each of the PCE generators and thus denoted as $\mathcal{G}_{\vec{\alpha}}$ (see Figs. 4 and 5). The proof is simplified if one uses the Kraus representation developed in Sec. V, so we postpone the demonstration to Appendix D. For single qubits, the identity corresponds to $\mathcal{G}_0$, shown in Fig. 1(b), whereas $\mathcal{G}_3$ is shown in Fig. 1(c). The two-qubit PCE generator represented in Fig. 3(c) acts on the first qubit (first column) as a map of its Bloch sphere to the x axis, and on the second qubit (first row) as an identity, hence it is labeled $\mathcal{G}_{(1,0)}$. See Fig. 5 for the notation of all two-qubit PCE generators.

A reflection symmetry is identified for PCE generators. Consider the map $\Sigma^{(k)}$ that reflects a multi-index $\vec{\alpha}$ with respect to the kth axis. This map leaves all components of $\vec{\alpha}$ invariant, except the kth component, which is transformed

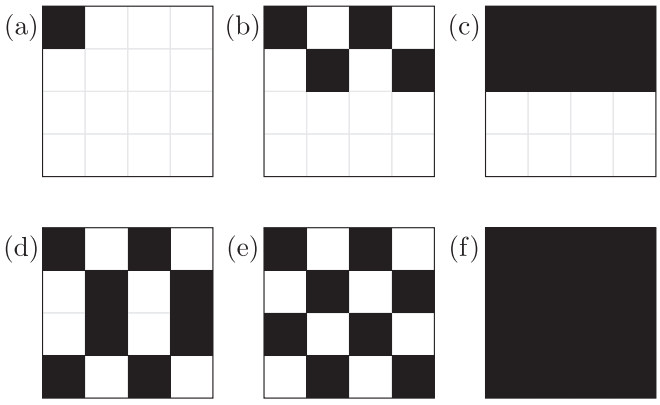

FIG. 3. Examples of diagrams for several two-qubit PCE quantum channels: (a) the totally depolarizing channel and (b) a PCE channel that preserves four components—the normalization component, one local component of qubit 2, and two correlations between the two qubits. (c), (d), and (e) show the three generators $\mathcal{G}_{(1,0)}$, $\mathcal{G}_{(3,2)}$, and $\mathcal{G}_{(2,2)}$, respectively; the combination (overlap of diagrams) of any two of them yields the channel in (b). (f) represents the identity map.

according to

$$0 \mapsto 3, \quad 3 \mapsto 0, \quad 1 \mapsto 2, \quad 2 \mapsto 1. \tag{28}$$

The maps have the following properties:

(1) $\Sigma^{(k)}(\vec{\alpha}) \oplus \Sigma^{(k)}(\vec{\beta}) = \vec{\alpha} \oplus \vec{\beta}$.

(2) $\Sigma^{(k)}(\vec{\alpha}) \neq \vec{\alpha}$.

From the first property, we now obtain

$$\vec{\alpha} = \Sigma^{(k)}(\vec{\alpha}) \oplus \Sigma^{(k)}(\vec{0}). \tag{29}$$

This implies that if $\Sigma^{(k)}(\vec{0})$ belongs to a channel then $\tau_{\vec{\alpha}} = \tau_{\Sigma^{(k)}(\vec{\alpha})}$, where we used the fact that for channels the nonzero elements are closed under $\oplus$. In other words, the components of a PCE channel are symmetric under reflection over the kth axis. Now consider the case in which $\Sigma^{(k)}(\vec{0})$ does not belong to generator. Then $\tau_{\vec{\alpha}} \neq \tau_{\Sigma^{(k)}(\vec{\alpha})}$, since the case $\tau_{\vec{\alpha}} = \tau_{\Sigma^{(k)}(\vec{\alpha})} = 1$ is forbidden due to Eq. (28) and the case $\tau_{\vec{\alpha}} = \tau_{\Sigma^{(k)}(\vec{\alpha})} = 0$ is also forbidden because for generators the codimension of the associated vector space is 1. This means that the components of a PCE channel are antisymmetric with respect to reflection over the kth axis. Indeed, the two-qubit PCE generators $\mathcal{G}_{(1,0)}$, $\mathcal{G}_{(3,2)}$, and $\mathcal{G}_{(2,2)}$ represented in Figs. 2(c), 2(d) and 2(e), respectively, are either symmetric or antisymmetric under reflection with respect to lines that divide the diagram in half vertically and horizontally.

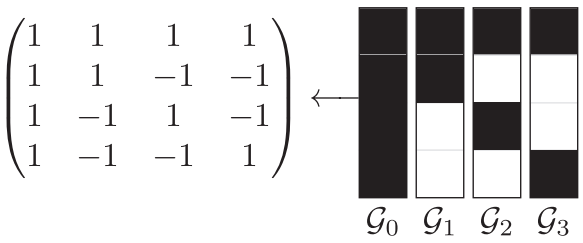

FIG. 4. The connection between rows or columns of a and single-qubit PCE generators $\mathcal{G}_\alpha$ is shown. One can identify the -1s of a with zeros in the sets $\{\tau_\alpha\}$ of preserved and erased components of each $\mathcal{G}_\alpha$. For any number of particles, such a simple relation holds see Sec. IV and Appendix D.

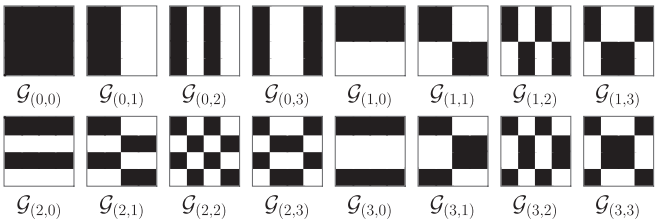

FIG. 5. PCE generators for two qubits. Notice that all generators are either symmetric or antisymmetric under horizontal and vertical reflections.

Finally, it is worth pointing out that A (and thus a) [see Eq. (15)] encodes all the information of PCE generators $\mathcal{G}_{\vec{\alpha}}$ and, therefore, of all PCE quantum channels. From A, the tensor power of matrix a, one can infer the components $\{\tau_{\vec{\alpha}}\}$ of a PCE generator $\mathcal{G}_{\vec{\alpha}}$ by taking row (or column) $\vec{\alpha}$ of A and replacing -1 with 0. The proof of the connection between PCEGs and A is given in Appendix D, and in Fig. 4 we illustrate this connection for the single-qubit case.

V. PCE CHANNELS AND DECOHERENCE

Lindblad processes arise naturally in many theoretical [15,30,39–42] and experimental [43] settings and are archetypical in decoherence dynamics. Moreover, these processes lead to a monotonic (continuous) loss of information [44] and describe noninvertible channels in the asymptotic limit $t \to \infty$ [this can be seen from the monotonic (continuous) decrease of the determinant (see Ref. [30])]. It is known that not every quantum channel can be seen as a snapshot of a process arising from a traditional Lindblad equation or even a time-dependent Lindblad equation [15,30]. Therefore, an interesting question is whether PCE channels can be seen as limit points of some Markovian processes. In this section we prove that in fact they are, and give two examples of Markovian implementations. The first of them consists in identifying each PCE channel as a fixed point of some pure dissipative process, and in the second implementation we relate each PCE channel to fixed points of some memoryless collision model.

A. Kraus representation

To derive the aforementioned implementations, we exploit the existence of the PCEGs and their *Kraus representation* (or operator-sum representation) which, for an arbitrary channel $\mathcal{E}$, reads

$$\mathcal{E}[\rho] = \sum_i K_i \rho K_i^\dagger, \tag{30}$$

with $\sum_i K_i^\dagger K_i = \mathbb{1}$ (the trace-preserving condition) [45]. Inspection of the Kraus operators for two-qubit PCEGs leads to the ansatz that the Kraus operators for the generator of $\mathcal{G}_{\vec{\alpha}}$ are

$$K_0 = \frac{\mathbb{1}}{\sqrt{2}}, \quad K_1 = \frac{\sigma_{\vec{\alpha}}}{\sqrt{2}}, \tag{31}$$

since the Kraus operators corresponding to a single-qubit PCE are $\{\mathbb{1}/\sqrt{2}, \sigma_\alpha/\sqrt{2}\}$, corresponding to the operation that

leaves the component σ_α invariant [6]. Notice that according to Kraus operators the generators $\mathcal{G}_{\vec{\alpha}}$ are N-qubit flip channels with flip probability $1/2$, where the joint flip is $\rho \mapsto \sigma_{\vec{\alpha}}\rho\sigma_{\vec{\alpha}}$. In fact, tracing out all particles except the kth one gives the well-known qubit flip channels, i.e., $\mathrm{tr}_{\not k}\mathcal{G}_{\vec{\alpha}} = \mathcal{G}_{\alpha_k}$ [see Eq. (D1)]. More generally, tracing out m particles leaves a $N-m$ particles flip channel (completely dephasing).

We shall first show that the Kraus operators in Eq. (31) produce a PCE. Notice that $\sigma_\alpha\sigma_\beta\sigma_\alpha = a_{\alpha\beta}\sigma_\beta$ [see Eq. (10)], which in turn implies that

$$\sigma_{\vec{\alpha}}\sigma_{\vec{\beta}}\sigma_{\vec{\alpha}} = A_{\vec{\alpha}\vec{\beta}}\sigma_{\vec{\beta}}. \tag{32}$$

Next, consider the action of a channel with Kraus representation (31) on a N-qubit system:

$$\begin{aligned}\rho \mapsto& \frac{1}{2^N}\sum_{\vec{\beta}} r_{\vec{\beta}}\left(\frac{1}{2}\sigma_{\vec{\beta}} + \frac{1}{2}\sigma_{\vec{\alpha}}\sigma_{\vec{\beta}}\sigma_{\vec{\alpha}}\right)\\ =& \frac{1}{2^N}\sum_{\vec{\beta}} r_{\vec{\beta}}\frac{1+A_{\vec{\alpha}\vec{\beta}}}{2}\sigma_{\vec{\beta}}.\end{aligned} \tag{33}$$

However, since $A_{\vec{\alpha}\vec{\beta}} = \pm 1$, the channel characterized by the Kraus operators in Eq. (31) is a PCE channel. Moreover, one can notice that, except for the first row, half of the matrix elements of each row are $+1$ and half are -1, which implies that the channel is a PCEG.

Observe also that a different choice of $\vec{\alpha}$ in Eq. (31) leads to different channels. This follows from the fact that if two channels were the same this would imply that the matrix representation of the corresponding superoperator of $\rho \mapsto \sigma_{\vec{\alpha}}\rho\sigma_{\vec{\alpha}}$ would have to be the same, which is clearly false. Since there are 4^n different $\vec{\alpha}$ values, this implies that all PCEGs (plus the identity map) are in one-to-one correspondence.

B. Pure dissipative implementation

In this section we show that any PCE channel can be seen as the fixed point of some decoherence process, starting with PCEGs and then extending to more general channels. Consider the following dynamical process that implements $\mathcal{G}_{\vec{\alpha}}$ when $t \to \infty$:

$$\begin{aligned}\mathcal{G}_{\vec{\alpha},t}[\rho] &= e^{-\gamma t}\rho + (1-e^{-\gamma t})\mathcal{G}_{\vec{\alpha}}[\rho]\\ &= \frac{(1+e^{-\gamma t})}{2}\rho + \frac{(1-e^{-\gamma t})}{2}\sigma_{\vec{\alpha}}\rho\sigma_{\vec{\alpha}},\end{aligned} \tag{34}$$

where $\gamma > 0$. It is easy to show that the family of channels $\mathcal{G}_{\vec{\alpha},t}$ parametrized with $t \geqslant 0$ forms a one-parametric semigroup, i.e., $\mathcal{G}_{\vec{\alpha},t_1}\mathcal{G}_{\vec{\alpha},t_2} = \mathcal{G}_{\vec{\alpha},t_1+t_2}$. Therefore $\mathcal{G}_{\vec{\alpha},t}$ describes a dissipative time-homogeneous Markovian process, which is always characterized by some Lindblad generator [39]. The Lindblad generator of $\mathcal{G}_{\vec{\alpha},t}$, denoted by $\mathcal{L}_{\vec{\alpha}}$, can be obtained using the standard procedure:

$$\mathcal{L}_{\vec{\alpha}}[\rho] = \left.\frac{d\mathcal{G}_{\vec{\alpha},t}[\rho]}{dt}\right|_{t=0} = \frac{\gamma(\sigma_{\vec{\alpha}}\rho\sigma_{\vec{\alpha}} - \rho)}{2}, \tag{35}$$

where the unique Lindblad operator associated with the relaxation ratio $\gamma/2$ is simply $\sigma_{\vec{\alpha}}$. Notice that $\sigma_{\vec{\alpha}}$ is traceless, therefore the process is purely dissipative [30].

Since PCEGs commute, we can describe easily any other PCE channel as a fixed point of a decoherence process. For them, the Lindblad generators are the sum of the Lindbladians of the corresponding generators. As an example, consider the channel depicted in Fig. 2(b); it is equal to $\mathcal{G}_{(0,3)}\mathcal{G}_{(3,3)}$, therefore it is the fixed point of the dissipation process described with the following Lindbladian:

$$\mathcal{L}[\rho] = \frac{\gamma_{(0,3)}(\sigma_{(0,3)}\rho\sigma_{(0,3)} - \rho)}{2} + \frac{\gamma_{(3,3)}(\sigma_{(3,3)}\rho\sigma_{(3,3)} - \rho)}{2}, \tag{36}$$

where $\gamma_{(0,3)}$ and $\gamma_{(3,3)}$ are positive and correspond to the Lindblad operators $\sigma_{(0,3)}$ and $\sigma_{(3,3)}$. Notice that such election of Lindblad operators is not unique, as the PCE channel described here is also equal to $\mathcal{G}_{(0,3)}\mathcal{G}_{(3,0)}$.

C. Collision model implementation

We show now that PCE channels can also be implemented with *simple collision models* [46]. To do this, observe that employing the Stinespring dilation theorem [47] PCEGs can be implemented using a unitary over the system and an ancilla. Since PCEGs always have Kraus rank 2, one can always choose a qubit as the ancillary system. Concretely,

$$\mathcal{G}_{\vec{\alpha}}[\rho] = \mathrm{tr}_{\mathrm{qubit}}[U_{\vec{\alpha}}(\rho\otimes|0\rangle\langle 0|)U_{\vec{\alpha}}^\dagger], \tag{37}$$

where $\mathrm{tr}_{\mathrm{qubit}}$ denotes the partial trace over the ancillary qubit, with the unitary defined as follows:

$$U_{\vec{\alpha}}|\psi\rangle|0\rangle = \frac{1}{\sqrt{2}}(|\psi\rangle|0\rangle + \sigma_{\vec{\alpha}}|\psi\rangle|1\rangle), \tag{38}$$

$$U_{\vec{\alpha}}|\psi\rangle|1\rangle = \frac{1}{\sqrt{2}}(|\psi\rangle|0\rangle - \sigma_{\vec{\alpha}}|\psi\rangle|1\rangle). \tag{39}$$

Therefore, any concatenation of PCEGs can be described as a collision model with as many collisions as generators needed. In fact, generators are described with one collision. For the general case consider some PCE channel $\mathcal{E}$ generated with $\{\mathcal{G}_{\vec{\alpha}_1}, \mathcal{G}_{\vec{\alpha}_2}, \ldots, \mathcal{G}_{\vec{\alpha}_M}\}$. For this we can define an environment consisting of M qubits initially in the state $(|0\rangle\langle 0|)^{\otimes M}$, or equivalently one qubit with the additional assumption that its state is reset to $|0\rangle$ after each collision (memoryless collisions). The collision with the k-th particle is described by $U_{\vec{\alpha}_k}$, which acts solely over the system and the kth particle. Therefore $\mathcal{E}$ can be written as follows:

$$\mathcal{E}[\rho] = \mathrm{tr}_{\mathrm{E}}\left[\left(U_{\vec{\alpha}_1}\ldots U_{\vec{\alpha}_M}\right)\rho\otimes(|0\rangle\langle 0|)^{\otimes M}\left(U_{\vec{\alpha}_1}\ldots U_{\vec{\alpha}_M}\right)^\dagger\right], \tag{40}$$

where tr_{E} is the partial trace over all ancillary qubits. Notice that as PCEGs commute the order of the collisions is irrelevant.

VI. CONCLUSIONS AND OUTLOOK

In this paper we introduce and characterize a set of quantum maps which either preserve or completely erase the components of a multiqubit density matrix, in the basis of Pauli strings; we call those maps *Pauli component erasing maps*. For a single qubit these include the completely depolarizing and dephasing channels. To start the characterization, we note that not all PCE maps are quantum channels, as some are not completely positive. In fact, the most laborious task of this paper was to evaluate complete positivity conditions given by the Choi-Jamiokowski isomorphism, after which we

showed that the components of PCE quantum channels form a finite vector space. This in turn allows us to unravel several properties, such as the possible number of PCE channels and the number of components preserved, while also providing advantages to study numerically this set, for example, by implying an efficient method to construct all quantum channels for a given number of qubits.

Similar to other objects in open quantum systems (for example, Lindblad processes), PCE quantum channels form a semigroup, but finite in this case. For PCE channels, the generators are generalized flip operations, i.e., channels that with probability $1/2$ apply a joint flip. This structure allows us to link this channel with multiqubit decoherence processes which can be described, say, by simple dissipative processes or memoryless collision models, which in turn may pave a way to either implement these channels or connect them with already existing decoherence families. This, together with the discovered algebraic structure that translates complete positivity into an explicit conditioned preservation of many-body correlations, encompasses an advance in the knowledge of the mathematical structures underlying general quantum channels.

In the future we might consider generalizations (such as going from qubits to qudits) as well as the geometric role of PCE channels within the set of all quantum channels to further advance the understanding of open quantum systems. We have thus described a family of quantum channels with a very special mathematical structure that allows us to widen the understanding of quantum channels in the context of many-body systems.

ACKNOWLEDGMENTS

Support by CONACyT Grants No. 285754 and No. 254515 and UNAM-PAPIIT Grants No. IG100518 and No. IG101421 is acknowledged. J.A.d.L. acknowledges a scholarship from CONACyT. J.A.d.L. thanks Juan Diego Chang for the fruitful discussions and support at the early stages of this project. A.F. acknowledges funding by Fundação de Amparo à Ciência e Tecnologia do Estado de Pernambuco, through Grants No. BFP-0168-1.05/19 and No. BFP-0115-1.05/21. D.D. acknowledges OPTIQUTE Grant No. APVV-18-0518, DESCOM Grant No. VEGA-2/0183/21, and the Štefan Schwarz Support Fund.

APPENDIX A: QUANTUM-CLASSICAL CHANNELS

A quantum-classical (QC) channel is defined by using an orthonormal basis in the Hilbert space. Let $B = \{|\psi_i\rangle\}$ be such a basis in H with $\dim(\mathsf{H}) = 2^N$; the QC channel associated to B is

$$\mathcal{E}_B^{\mathrm{QC}}[\rho] = \sum_{i=1}^{2^N} \langle\psi_i|\rho|\psi_i\rangle |\psi_i\rangle\langle\psi_i|, \tag{A1}$$

that is, QC channels project density matrices onto the corresponding diagonal matrix in the basis B [22].

Consider now that the basis B is the simultaneous eigenbasis of a maximal set of commuting Pauli strings denoted by set(B); such a set contains 2^N elements (including the identity), and there are $2^N + 1$ of such sets [29]. Now we proceed to demonstrate that the QCs defined in this way are PCE channels with 2^N 1s on their diagonal.

First we compute the components of $\mathcal{E}_B^{\mathrm{QC}}$ in the basis $2^{-N/2}\{\sigma_{\vec{\alpha}}\}$:

$$\left(\mathcal{E}_B^{\mathrm{QC}}\right)_{\vec{k}\vec{l}} = \frac{1}{2^N}\sum_{i=1}^{2^N} \langle\psi_i|\sigma_{\vec{k}}|\psi_i\rangle\langle\psi_i|\sigma_{\vec{l}}|\psi_i\rangle. \tag{A2}$$

To evaluate the components, observe that $\langle\psi_i|\sigma_{\vec{k}}|\psi_i\rangle^2 = 1 \ \forall\sigma_{\vec{k}} \in \mathrm{set}(B)$, and from the formula for the purity of $|\psi_i\rangle$,

$$1 = \frac{1}{2^N}\sum_{\vec{k}} \langle\psi_i|\sigma_{\vec{k}}|\psi_i\rangle^2, \tag{A3}$$

it follows that $\langle\psi_i|\sigma_{\vec{k}'}|\psi_i\rangle = 0 \ \ \forall\sigma_{\vec{k}'} \notin \mathrm{set}(B)$ since there are only positive terms in the sum, and 2^N of them are already equal to 1. Therefore,

$$\begin{aligned}&\left(\mathcal{E}_B^{\mathrm{QC}}\right)_{\vec{k}\vec{k}} = 1,\\ &\left(\mathcal{E}_B^{\mathrm{QC}}\right)_{\vec{k}\vec{l}'} = \left(\mathcal{E}_B^{\mathrm{QC}}\right)_{\vec{l}'\vec{l}'} = 0 \ \ \forall\sigma_{\vec{k}} \in \mathrm{set}(B) \ \ \forall\sigma_{\vec{l}'} \notin \mathrm{set}(B).\end{aligned} \tag{A4}$$

To compute $\left(\mathcal{E}_B^{\mathrm{QC}}\right)_{\vec{k}\vec{l}}$ for $\sigma_{\vec{k}}, \sigma_{\vec{l}} \in \mathrm{set}(B)$ with $\vec{k} \neq \vec{l}$, observe that $\left(\mathcal{E}_B^{\mathrm{QC}}\right)_{\vec{k}\vec{l}} = \left(\mathcal{E}_B^{\mathrm{QC}}\right)_{\vec{l}\vec{k}}$, i.e., the matrix corresponding to $\mathcal{E}^{\mathrm{QC}}$ is an orthogonal projector. Thus, considering the block,

$$\begin{bmatrix}\left(\mathcal{E}_B^{\mathrm{QC}}\right)_{\vec{k}\vec{k}} & \left(\mathcal{E}_B^{\mathrm{QC}}\right)_{\vec{k}\vec{l}}\\ \left(\mathcal{E}_B^{\mathrm{QC}}\right)_{\vec{k}\vec{l}} & \left(\mathcal{E}_B^{\mathrm{QC}}\right)_{\vec{l}\vec{l}}\end{bmatrix} = \begin{bmatrix}1 & \left(\mathcal{E}_B^{\mathrm{QC}}\right)_{\vec{k}\vec{l}}\\ \left(\mathcal{E}_B^{\mathrm{QC}}\right)_{\vec{k}\vec{l}} & 1\end{bmatrix}, \tag{A5}$$

it is easy to check that the latter is a projector only if $\left(\mathcal{E}_B^{\mathrm{QC}}\right)_{\vec{k}\vec{l}} = 0$. Since there are exactly 2^N elements of the form $\left(\mathcal{E}_B^{\mathrm{QC}}\right)_{\vec{k}\vec{k}}$ with $\sigma_{\vec{k}} \in \mathrm{set}(B)$, then the channel $\mathcal{E}_B^{\mathrm{QC}}$ is PCE with 2^N 1s on its diagonal.

APPENDIX B: DIAGONALIZATION OF CHOI MATRIX $\mathcal{D}_N$

In order to simplify the derivation of the relations, let us employ pairs of binary indices instead of a single quaternary, i.e., $\alpha \to j + 2k$. For the sake of clarity, we use Latin symbols for binary indices, and reserve Greek letters for quaternary ones. We can write the elements of the Pauli basis $(\sigma_0, \sigma_1, i\sigma_2, \sigma_3)$, compactly as $\sigma_{kl} = \sum_{j=0}^{1}(-1)^{jk}|j\rangle\langle j + l(\mathrm{mod}2)|$. In vectorized form

$$|\sigma_{kl}\rangle\!\rangle = \sum_{j=0}^{1}(-1)^{jk}|j\rangle|j + l(\mathrm{mod}\,2)\rangle, \tag{B1}$$

and its inverse relation

$$|k\rangle|k + l(\mathrm{mod}\,2)\rangle = \frac{1}{2}\sum_{j=0}^{1}(-1)^{jk}\,|\sigma_{jl}\rangle\!\rangle\,. \tag{B2}$$

On the other hand, the matrix form of an arbitrary Pauli map $\mathcal{E}$ may be written as

$$\hat{\mathcal{E}} = \frac{1}{2}\sum_{lm=0}^{1}\tau_{lm}\,|\sigma_{lm}\rangle\!\rangle\langle\!\langle\sigma_{lm}| \tag{B3}$$

$$= \frac{1}{2}\sum_{jklm}\tau_{lm}(-1)^{l(j+k)} \times |j\rangle|j + m(\mathrm{mod}\,2)\rangle\langle k|\langle k + m(\mathrm{mod}\,2)|. \tag{B4}$$

After applying the reshuffling operation on $\hat{\mathcal{E}}$, we obtain the Choi matrix associated to the map. It reads

$$\mathcal{D} = \frac{1}{2}\sum_{jklm} \tau_{lm}(-1)^{l(j+k)} \times |j\rangle|k\rangle\langle j+m(\mathrm{mod}2)|\langle k+m(\mathrm{mod}2)|. \quad \text{(B5)}$$

Note furthermore that the expression above may also be written as a combination of tensor products of Pauli matrices:

$$\mathcal{D} = \frac{1}{2}\sum_{lm} \tau_{lm}\sigma_{lm}\otimes\sigma^*_{lm}. \quad \text{(B6)}$$

Returning to Eq. (B5), let us apply the index relabeling $k \to j+k(\mathrm{mod}2)$; then the Choi matrix reads

$$\mathcal{D} = \frac{1}{2}\sum_{jklm} \tau_{lm}(-1)^{lk} \times |j\rangle|j+k(\mathrm{mod}\,2)\rangle\langle j+m(\mathrm{mod}\,2)|\langle j+m+k(\mathrm{mod}\,2)|, \quad \text{(B7)}$$

since $(-1)^{j+(j+k(\mathrm{mod}2))} = (-1)^k$. To continue, we use the relation between computational and Pauli elements [Eq. (B2)], and notice that $\sum_j (-1)^{j(m\pm n)} = 2\delta_{mn}$. We arrive to the simple expression

$$\mathcal{D} = \frac{1}{2}\sum_{jk}\left(\frac{1}{2}\sum_{lm}(-1)^{jm+kl}\tau_{lm}\right)|\sigma_{jk}\rangle\!\rangle\langle\!\langle\sigma_{jk}|\,. \quad \text{(B8)}$$

Notice that $\mathcal{D}$ is already written in its diagonal form, and one can identify by inspection the eigenvalues. The eigenvalues read

$$\lambda_{jk} = \frac{1}{2}\sum_{lm}(-1)^{jm+kl}\tau_{lm}, \quad \text{(B9)}$$

or more compactly $\vec{\lambda} = (1/2)H\otimes H\vec{\tau}$, where H is the Hadamard matrix.

For the sake of convenience in the demonstration of several useful properties of the PCE channels, we shall reorder the eigenvalues, to write

$$\lambda = \tfrac{1}{2}a\tau \quad \text{(B10)}$$

with a the matrix shown in Eq. (10) instead of $H\otimes H$. This can be done due to the fact that both matrices (a and $H\otimes H$) are equivalent up to a permutation of rows. In other words this operation corresponds to a reordering of the eigenvalues.

N qubits

To work out the N-qubit case, we again rely on binary indices. In this case, we replace N-dimensional vector $\vec{\alpha}$ with a pair of N-dimensional vector binary indices $\vec{j}$ and $\vec{k}$ so that each entry α_i of $\vec{\alpha}$ is identified with the pair j_i and k_i as in the single-qubit case of the previous subsection. Then, all the steps leading to Eq. (B9) can be redone.

The tensor product of Pauli matrices, in vector form, will be denoted by $|\sigma_{\vec{k}\vec{l}}\rangle\!\rangle$. With this in mind, a N-qubit Pauli map can be written as

$$\hat{\mathcal{E}}_N = \frac{1}{2^N}\sum_{\vec{l}\vec{m}} \tau_{\vec{l}\vec{m}}\,|\sigma_{\vec{l}\vec{m}}\rangle\!\rangle\langle\!\langle\sigma_{\vec{l}\vec{m}}|\,. \quad \text{(B11)}$$

The generalizations of Eqs. (B1) and (B2) read

$$|\sigma_{\vec{k}\vec{l}}\rangle\!\rangle = \sum_{\vec{j}}(-1)^{\vec{j}\cdot\vec{k}}|\vec{j}\rangle|\vec{j}+\vec{l}(\mathrm{mod}2)\rangle, \quad \text{(B12)}$$

$$|\vec{l}\rangle|\vec{l}+\vec{n}(\mathrm{mod}2)\rangle = \frac{1}{2^N}\sum_{\vec{m}}(-1)^{\vec{m}\cdot\vec{l}}\,|\sigma_{\vec{m}\vec{n}}\rangle\!\rangle\,. \quad \text{(B13)}$$

By employing the previous relations, we can write the matrix representation of the map, $\hat{\mathcal{E}}_N$ in the N-qubit computational basis, as

$$\hat{\mathcal{E}} = \frac{1}{2}\sum_{\vec{j}\vec{k}\vec{l}\vec{m}} \tau_{\vec{l}\vec{m}}(-1)^{\vec{l}(\vec{j}+\vec{k})} \times |\vec{j}\rangle|\vec{j}+\vec{m}(\mathrm{mod}2)\rangle\langle\vec{k}|\langle\vec{k}+\vec{m}(\mathrm{mod}2)|. \quad \text{(B14)}$$

In this way it is straightforward to apply the reshuffling operation on $\hat{\mathcal{E}}_N$ to obtain the associated Choi matrix, and then transform back to the Pauli basis and simplify to obtain

$$\mathcal{D}_N = \frac{1}{2^N}\sum_{\vec{m}\vec{n}}\left(\frac{1}{2^N}\sum_{\vec{l}\vec{m}}\tau_{\vec{l}\vec{m}}(-1)^{\vec{l}\cdot\vec{n}+\vec{m}\cdot\vec{m}}\right)|\sigma_{\vec{m}\vec{n}}\rangle\!\rangle\langle\!\langle\sigma_{\vec{m}\vec{n}}|\,. \quad \text{(B15)}$$

All intermediate steps, from Eq. (B3) to Eq. (B8) are similar, but with a vectorized version of the indices, and appropriate normalization constants. Again, we are left with an expression that displays explicitly the eigenvalues of the Choi matrix, so we can write

$$\lambda_{\vec{j}\vec{k}} = \frac{1}{2^N}\sum_{\vec{l}\vec{m}}(-1)^{\vec{j}\cdot\vec{m}+\vec{k}\cdot\vec{l}}\tau_{\vec{l}\vec{m}} \quad \text{(B16)}$$

or more compactly $\lambda = (H\otimes H/2)^{\otimes N}\tau$. Again, we prefer to reorganize the indices to be able to write

$$\lambda = \frac{1}{2^N}A\tau, \quad \text{(B17)}$$

where $A = a^{\otimes N}$.

APPENDIX C: NUMBER OF PCE'S FOR A FIXED NUMBER OF INVARIANT COMPONENTS

Finally, we may enumerate straightforwardly the subspaces W of dimension K. We do this in two steps: first, we evaluate $\mathcal{N}_{K,N}$, the number of all linearly independent subsets V with K elements. Each of these is the basis of one subspace of dimension K, but each subspace has a number $\mathcal{M}_K$ of different bases. The crucial point is that $\mathcal{M}_K$ is independent of the subspace under consideration: $\mathcal{M}_K$ simply describes the number of linear maps of W onto itself. The total number $\mathcal{S}_{N,K}$ of subspaces of dimension K is therefore $\mathcal{N}_{N,K}/\mathcal{M}_K$.

To evaluate $\mathcal{N}_{N,K}$ we proceed by steps: the first element of the basis can be any nonzero element, of which the number is $2^{2N}-1$. For the basis element $m+1$, we must choose from those which do not belong to the m-dimensional space generated by the first m basis elements, so that one chooses from $2^{2N}-2^m$. We thus have

$$\mathcal{N}_{N,K} = \prod_{m=0}^{K-1}(2^{2N}-2^m). \quad \text{(C1)}$$

On the other hand, any map of a K-dimensional vector space W onto itself is uniquely defined by a nonsingular binary $K \times K$ matrix over the field $\{0, 1\}$. To count these, we proceed as above: the first line is an arbitrary nonzero vector, of which there are $2^K - 1$. For the row $m + 1$ we must choose an arbitrary vector not belonging to those generated by the first m vectors, of which there are $2^K - 2^m$. This eventually yields

$$\mathcal{M}_K = \prod_{m=0}^{K-1} (2^K - 2^m). \tag{C2}$$

From this it follows that

$$\mathcal{S}_{N,K} = \prod_{m=0}^{K-1} \frac{2^{2N-m} - 1}{2^{K-m} - 1}. \tag{C3}$$

APPENDIX D: LOCAL ACTION AND LABELING OF PCE GENERATORS

The local action of a generator $\mathcal{G}_{\vec{\alpha}}$ on every qubit in the system depends only, as its notation suggests, on the multi-index $\vec{\alpha}$. This index has a simple meaning that can be read from the graphical representation of the channel. Recall the single-qubit PCE generators, shown in Fig. 4, denoted by $\mathcal{G}_0$ (corresponding to the identity map) and $\mathcal{G}_{1,2,3}$ (corresponding to the completely bit, phase, and bit-phase flip channels, respectively). One can easily read the diagrams in the following manner: $\alpha = 0$ corresponds to all squares black, whereas for $\alpha > 0$ we have only the zeroth and the αth squares black. Let us generalize this characterization rule for N-qubit PCE generators. Consider that the reduced density matrix of the kth qubit after generator $\mathcal{G}_{\vec{\alpha}}$ acts on the entire system

$$\begin{aligned} \mathrm{tr}_{\not k}\mathcal{G}_{\vec{\alpha}}[\rho] &= \frac{1}{2}\mathrm{tr}_{\not k}(\rho + \sigma_{\vec{\alpha}}\rho\sigma_{\vec{\alpha}}) = \frac{\rho_k}{2} + \frac{\sigma_{\alpha_k}\rho_k\sigma_{\alpha_k}}{2} \\ &= \mathcal{G}_{\alpha_k}[\rho_k], \end{aligned} \tag{D1}$$

where $\not k$ means that all qubits except for the kth one are traced out. We can read from (D1) that α_k not only characterizes $\mathcal{G}_{\alpha_k}$ but actually tells us which single-qubit channel is acting locally on the kth qubit. The action of $\mathcal{G}_{\alpha_k}$ on the local components of the reduced density matrix ρ_k reads $r_{0,\ldots,j_k,\ldots,0} \mapsto \tau_{0,\ldots,j_k,\ldots,0} r_{0,\ldots,j_k,\ldots,0}$. The general characterization rule for all PCE generators $\mathcal{G}_{\vec{\alpha}}$ is clear now: if all $\tau_{0,\ldots,j_k,\ldots,0} = 1$, then $\alpha_k = 0$; otherwise, if $\tau_{0,\ldots,j_k,\ldots,0} = 1$ (with $j_k > 0$), then $\alpha_k = j_k$. For two-qubit PCE diagrams this means that the multi-index $\vec{\alpha}$ is encoded in the first column and row of the diagrams (see $\mathcal{G}_{(0,2)}$ in Fig. 5), all $\tau_{j_1,0} = 1$ and $\tau_{(0,2)} = 1$, and then $\vec{\alpha} = (0, 2)$. In Fig. 5 we show all two-qubit PCE generators and their corresponding notation $\mathcal{G}_{\vec{\alpha}}$.

An interesting relation of the generators and the A matrix can be derived with the tools developed. Consider the generator $\mathcal{G}_{\vec{\alpha}}$, and its Pauli components $\tau_{\vec{\beta}}^{(\vec{\alpha})}$. We can calculate the former studying the action of the generator on the non-normalized state $\varrho = \sum_{\vec{\gamma}} \sigma_{\vec{\gamma}}$. Let us proceed with such calculation, using the Kraus decomposition Eq. (31):

$$\tau_{\vec{\beta}}^{(\vec{\alpha})} = \mathrm{tr}\sigma_{\vec{\beta}}\mathcal{G}_{\vec{\alpha}}[\varrho] \tag{D2}$$

$$= \frac{1}{2}\sum_{\vec{\gamma}} \mathrm{tr}[\sigma_{\vec{\beta}}\sigma_{\vec{\gamma}} + \sigma_{\vec{\beta}}\sigma_{\vec{\alpha}}\sigma_{\vec{\gamma}}\sigma_{\vec{\alpha}}] \tag{D3}$$

$$= \frac{1}{2}(1 + A_{\vec{\alpha}\vec{\beta}}) \tag{D4}$$

where we have used the orthogonality relations of Pauli matrices and Eq. (32). This means that one can read the αth generators directly from matrix A (see Fig. 4 for the $n = 1$ case). Alternatively one could construct the A matrix for $n = 2$, from Fig. 5, where the first row of this matrix is read from $\mathcal{G}_{(0,0)}$, replacing black (white) squares with 1s (-1s), the second row from $\mathcal{G}_{(0,1)}$, etc.

[1] J. S. Bell, Phys. Phys. Fiz. **1**, 195 (1964).
[2] S. Köhnke, E. Agudelo, M. Schünemann, O. Schlettwein, W. Vogel, J. Sperling, and B. Hage, Phys. Rev. Lett. **126**, 170404 (2021).
[3] H. Ollivier and W. H. Zurek, Phys. Rev. Lett. **88**, 017901 (2001).
[4] R. Horodecki, P. Horodecki, M. Horodecki, and K. Horodecki, Rev. Mod. Phys. **81**, 865 (2009).
[5] C. H. Bennett, G. Brassard, C. Crépeau, R. Jozsa, A. Peres, and W. K. Wootters, Phys. Rev. Lett. **70**, 1895 (1993).
[6] M. A. Nielsen and I. L. Chuang, *Quantum Computation and Quantum Information: 10th Anniversary Edition*, 10th ed. (Cambridge University, New York, 2011).
[7] F. Sapienza, F. Cerisola, and A. J. Roncaglia, Nat. Commun. **10**, 2492 (2019).
[8] M. Schlosshauer, Decoherence, the measurement problem, and interpretations of quantum mechanics, arXiv:0312059.
[9] G. J. Mooney, G. A. L. White, C. D. Hill, and L. C. L. Hollenberg, J. Phys. Commun. **5**, 095004 (2021).
[10] H.-J. Briegel, W. Dür, J. I. Cirac, and P. Zoller, Phys. Rev. Lett. **81**, 5932 (1998).
[11] C. H. Bennett, G. Brassard, S. Popescu, B. Schumacher, J. A. Smolin, and W. K. Wootters, Phys. Rev. Lett. **76**, 722 (1996).
[12] I. Georgescu, 25 years of quantum error correction (2020).
[13] B. M. Terhal, Rev. Mod. Phys. **87**, 307 (2015).
[14] G. Bacciagaluppi, in *The Stanford Encyclopedia of Philosophy*, edited by E. N. Zalta, Fall 2020 ed. (Metaphysics Research Lab, Stanford University, 2020).
[15] D. Davalos, M. Ziman, and C. Pineda, Quantum **3**, 144 (2019).
[16] M. B. Ruskai, S. Szarek, and E. Werner, Linear Algebra and Its Applications **347**, 159 (2002).
[17] H. Breuer and F. Petruccione, *The Theory of Open Quantum Systems* (Oxford University, New York, 2007).
[18] C. Duarte, G. D. Carvalho, N. K. Bernardes, and F. de Melo, Phys. Rev. A **96**, 032113 (2017).
[19] C. Pineda, D. Davalos, C. Viviescas, and A. Rosado, Phys. Rev. A **104**, 042218 (2021).
[20] T. Heinosaari and M. Ziman, *The Mathematical Language of Quantum Theory: From Uncertainty to Entanglement* (Cambridge University, New York, 2012).
[21] T. Rybár, S. N. Filippov, M. Ziman, and V. Bužek, J. Phys. B: At. Mol. Opt. Phys. **45**, 154006 (2012).

[22] M. Nathanson and M. B. Ruskai, J. Phys. A: Math. Theor. **40**, 8171 (2007).

[23] K. Siudzińska, Phys. Rev. A **102**, 032603 (2020), 2003.12570.

[24] I. Sergeev, Rep. Math. Phys. **83**, 349 (2019).

[25] D. Chruściński and K. Siudzińska, Phys. Rev. A **94**, 022118 (2016).

[26] H. Ohno and D. Petz, Acta Math Hung **124**, 165 (2009).

[27] A. Fonseca, Phys. Rev. A **100**, 062311 (2019).

[28] G. Kimura, Phys. Lett. A **314**, 339 (2003).

[29] J. Lawrence, Č. Brukner, and A. Zeilinger, Phys. Rev. A **65**, 032320 (2002).

[30] M. M. Wolf and J. I. Cirac, Commun. Math. Phys. **279**, 147 (2008).

[31] I. Bengtsson and K. Zyczkowski, *Geometry of Quantum States: An Introduction to Quantum Entanglement*, 2nd ed. (Cambridge University, New York, 2017).

[32] A. Jamiołkowski, Rep. Math. Phys. **3**, 275 (1972).

[33] M.-D. Choi, Linear Algebra and Its Applications **10**, 285 (1975).

[34] M. A. Nielsen and I. L. Chuang, *Quantum Computation and Quantum Information: 10th Anniversary Edition*, 10th ed. (Cambridge University, New York, 2011).

[35] A. Gilchrist, D. R. Terno, and C. Wood, arXiv:0911.2539.

[36] We can further unravel the vector space, by identifying each index $\alpha \in \{0, 1, 2, 3\}$ with its binary notation, e.g., identify 2 with (1,0), such that to each multi-index $\vec{\alpha}$ there corresponds a binary string of length $2N$. In fact, our sum $\oplus$ would correspond to addition modulo 2 of each of the $2N$ components.

[37] S. Roman, *Advanced Linear Algebra*, 3rd ed., Graduate Texts in Mathematics Vol. 135 (Springer, New York, 2008).

[38] D. Gottesman, Stabilizer codes and quantum error correction, Ph.D. thesis, California Institute of Technology, 1997.

[39] G. Lindblad, Commun. Math. Phys. **48**, 119 (1976).

[40] A. Kossakowski, Rep. Math. Phys. **3**, 247 (1972).

[41] A. Kossakowski, Bull. Acad. Pol. Sci. **20**, 1021 (1972).

[42] V. Gorini, A. Kossakowski, and E. C. G. Sudarshan, J. Math. Phys. **17**, 821 (1976).

[43] N. Boulant, T. F. Havel, M. A. Pravia, and D. G. Cory, Phys. Rev. A **67**, 042322 (2003).

[44] B. Vacchini, A. Smirne, E.-M. Laine, J. Piilo, and H.-P. Breuer, New J. Phys. **13**, 093004 (2011).

[45] *Ann. Phys.*, edited by K. Kraus, A. Böhm, J. D. Dollard, and W. H. Wootters, Lecture Notes in Physics Vol. 190 (Springer-Verlag, Berlin, 1983), p. 160.

[46] M. Ziman and V. Bužek, in *Quantum Dynamics and Information* (World Scientific, Singapore, 2010), pp. 199–227.

[47] W. F. Stinespring, Proc. Am. Math. Soc. **6**, 211 (1955).